

Pickering Emulsions of Fluorinated TiO₂: A New Route for Intensification of Photocatalytic Degradation of Nitrobenzene

Nidhal Fessi, Mohamed Faouzi Nsib, Yves Chevalier,* Chantal Guillard, Frédéric Dappozze, Ammar Houas, Leonardo Palmisano, and Francesco Parrino*



Cite This: *Langmuir* 2020, 36, 13545–13554



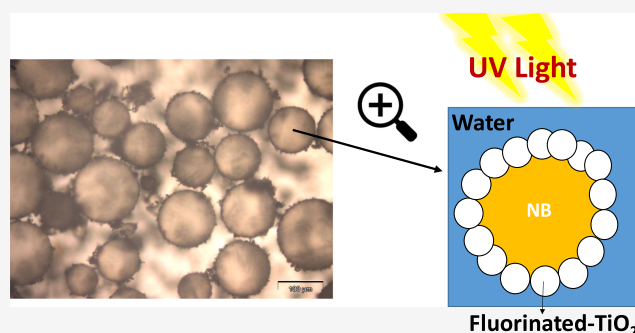
Read Online

ACCESS |

Metrics & More

Article Recommendations

ABSTRACT: Fluorination of the TiO₂ surface has been often reported as a tool to increase the photocatalytic efficiency due to the beneficial effects in terms of production of oxidizing radicals. Moreover, it is shown that the unique amphiphilic properties of the fluorinated TiO₂ (TiO₂-F) surface allow one to use this material as a stabilizer for the formulation of Pickering emulsions of poorly soluble pollutants such as nitrobenzene (NB) in water. The emulsions have been characterized in terms of size of the droplets, type of emulsion, possibility of phase inversion, contact angle measurements, and optical microscopy. The emulsified system presents micrometer-sized droplets of pollutant surrounded by the TiO₂-F photocatalyst. Consequently, the system can be considered



to be composed of microreactors for the degradation of the pollutant, which maximize the contact area between the photocatalyst and substrate. The enhanced photocatalytic activity of TiO₂-F was confirmed in the present paper as the apparent rate constants of NB photodegradation were 16×10^{-3} and $12 \times 10^{-3} \text{ min}^{-1}$ for fluorinated and bare TiO₂, respectively. At NB concentrations largely exceeding its solubility, the rate constant was $0.04 \times 10^{-3} \text{ min}^{-1}$ in the presence of both TiO₂ and TiO₂-F. However, unlike TiO₂, TiO₂-F stabilized NB/water emulsions and, under these conditions, the efficiency of NB photocatalytic degradation in the emulsified system was ca. 18 times higher than in the nonemulsified one. This result is relevant also in terms of practical applications because it opens the route to one-pot treatments of biphasic polluted streams without the need of preliminary physical separation treatments.

INTRODUCTION

Nitrobenzene (NB) is a toxic and biopersistent aromatic compound.¹ It affects the central nervous and cardiovascular systems, is suspected to be carcinogenic,² and poses serious concerns for its effects in the environment.^{3–6} However, NB is implemented in many industrial processes for the production of perfumes, resins, dyes, explosives, and pesticides.^{7–9} Therefore, it is often present not only in industrial wastewater streams but also in surface and ground water¹⁰ because its high chemical stability and low water solubility lead to its accumulation in the environment. Conventional purification and decontamination rely on physical treatments such as separation techniques.^{11,12} These methods are generally expensive, are poorly efficient, and afford only the removal of the pollutants without chemical degradation.

Photocatalysis is a promising advanced oxidation process that has been often proposed for water remediation applications as it allows oxidation of almost all harmful organic species. Upon absorption of light of suitable energy, reactive oxygen species (ROS) possessing high oxidizing ability are generated. The transfer of the photocatalytic process from the laboratory to real applications is a current

concern that deserves a great deal of research efforts. The photodegradation of poorly water-soluble substrates faces some problems whose solution still requires basic research. In these cases, polluted water cannot be directly used as in most photocatalytic applications¹³ because of the low concentration of the dissolved substrate and its low affinity with the generally hydrophilic surface of the photocatalyst. These factors negatively affect the quantum efficiency of the process and, consequently, its economic feasibility. The use of different solvents has been proposed to overcome these problems in cases where photocatalysis was used for organic synthesis purposes.¹⁴ For instance, the degradation of polycyclic aromatic hydrocarbons (PAHs) has been recently carried out in the green solvent dimethyl carbonate in the presence of a minimum amount of water necessary to induce

Received: August 4, 2020

Revised: October 1, 2020

Published: November 4, 2020



the formation of oxidizing radical species. Such a shift of solvent is better restricted to the synthesis of compounds with high added value. Using solvents other than water for environmental remediation faces hard problems of costs and management, especially in view of large-scale applications.

A different approach consists of the formation of emulsions of the hydrophobic pollutant dispersed in water in which the photocatalyst can also act as a stabilizer of the emulsion. In this way, the preliminary physical separation of the pollutant can be by-passed and the degradation reaction can take place inside microreactor-like droplets of the substrate surrounded (and stabilized) by the photocatalyst itself. This configuration is beneficial in terms of photocatalytic activity as it creates a larger contact area between the catalyst and pollutant, optimizes the availability of the active sites, and offers all of the advantages of working in micrometer-sized reactors.¹⁵

The organic pollutant plays the role of the “oil” in the emulsion. The emulsion can be obtained by applying external energy either in the form of mechanical stirring or sonication. When the emulsion is stabilized by solid nanoparticles located at the oil–water interface, a “Pickering emulsion”¹⁶ is obtained.

Pickering emulsions can be of the oil-in-water (O/W), water-in-oil (W/O), or even multiple types.^{17–19} They possess the basic properties of classical emulsions stabilized by soluble surfactants (emulsifiers).²⁰ However, the stabilization produced by solid particles confers specific properties. The high resistance to coalescence is the main benefit.^{21–23} Furthermore, Pickering emulsions are stable in a wide range of experimental conditions; in particular, they are not very affected by temperature variations, changes in the composition of the oil phase, and the pH of the aqueous phase.²⁴ This makes them useful in pharmaceutical,^{25,26} cosmetic,²⁷ and food industries.^{28,29} In 2010, the pioneering work by Crossley et al.³⁰ paved the way for catalytic reactions in Pickering emulsions.^{31–38} However, only a few examples of photocatalytic reactions carried out in Pickering emulsions have been reported.^{39–41} As far as we know, fluorinated TiO₂ has never been proposed for that purpose, while it is instead widely studied as a photocatalyst because of its higher photoactivity than pure TiO₂. Its high photoactivity has been mainly attributed to (i) the presence of a defective surface, which increases the lifetime of the photogenerated charges,⁴² (ii) the greater production of highly oxidizing hydroxyl radicals due to the better availability of photogenerated holes,⁴³ and (iii) the possible production of singlet oxygen.⁴⁴

Otherwise, the wettability by oils and water and the dynamics of water molecules on the fluorinated TiO₂ surface have been poorly studied. It has been proposed, for example, that fluorination gives rise to an increase in the Lewis acidic strength of Ti⁴⁺ surface sites, which retain adsorbed water molecules,⁴⁵ thereby increasing the hydrophilic character of the surface. Similar conclusions have also been reached by other authors.⁴⁶ UV irradiation increases the polarity of the surface.⁴⁷ However, Mino et al.⁴⁸ recently revealed the complexity of the topic by showing evidence of different behaviors of various exposed crystalline facets and the different contributions of bulk and surface doping. Interestingly, this study disclosed that the presence of terminal fluoride groups on the {001} facet of TiO₂ decreased the hydrophilicity of the material by ca. two times. Therefore, the physical chemistry of fluorinated TiO₂ in Pickering emulsions

is not trivial from a scientific point of view due to the complex interactions of its surface with water and oils.⁴⁹

We recently reported on the changes induced by surface fluorination on the morphological, structural, surface, and electronic features of TiO₂.⁵⁰ While surface fluorination does not affect the bulk structural properties and the morphology of TiO₂ nanoparticles, it induces significant changes in terms of surface and electronic properties. In particular, the surface charge turns more negative upon fluorination, and supplementary intraband-gap energy states located up to 1.3 eV above the valence band are generated by the local interaction of chemisorbed fluorine atoms with the semiconducting structure of TiO₂. The correlation between the optoelectronic features and the photocatalytic activity has been discussed.⁵⁰ The unique surface properties of fluorinated TiO₂ deserve further investigations and can be exploited for specific applications. For instance, their influence on the selectivity of the industrially relevant photocatalytic synthesis of high-added-value compounds has recently been demonstrated.⁵¹

This paper reports the influence of surface fluorination of a nanostructured sol–gel-derived TiO₂ material on the stability of nitrobenzene/water emulsions and on the consequent efficiency of the photocatalytic degradation of nitrobenzene under UV irradiation. Notably, the possibility to treat in one-pot biphasic polluted streams, without the need of costly physical separation processes upstream, is of practical relevance.

■ EXPERIMENTAL SECTION

Preparation of the Photocatalysts. TiO₂ nanoparticles were synthesized by using a facile sol–gel technique. Nineteen milliliters of titanium tetraisopropoxide (Ti[OCH(CH₃)₂]₄, 97%, Alfa Aesar) was added to 4 mL of methanol (MeOH, 99.9%, Aldrich) and the obtained solution was sonicated in an ultrasonic bath (Elma, T460/H, 35 kHz and 170 W). The hydrolysis process was then performed by adding dropwise 74 mL of deionized water under reflux and magnetic stirring. The obtained white gel was filtered and washed several times using ethanol and deionized water. The resulting powder was dried at 100 °C for 18 h to evaporate water and the volatile organic compounds. Finally, the powder, labeled simply as TiO₂, was calcined in a muffle furnace at 400 °C for 4 h. Fluorination of TiO₂ was carried out by dispersing 1 g of the synthesized TiO₂ nanoparticles into 50 mL of 4% sodium fluoride (NaF, p.a., Aldrich) aqueous solution at pH 3.2 (obtained by addition of HNO₃) and stirring the suspension at room temperature for 48 h. The nanoparticles were separated by centrifugation, washed several times with HNO₃ aqueous solutions at pH 3.2, and finally dried at 80 °C for 2 h. The resulting powder was labeled as TiO₂-F.

The amount of fluorine in samples was determined by means of ion chromatography after digestion dissolution of the TiO₂ material by fusion with potassium hydrogen sulfate and extraction of the melt with dilute sulfuric acid.⁵² Collected samples were then analyzed for F[−] anions using ion chromatography (930 Compact IC Flex, Metrohm, Switzerland) equipped with a chemical suppressor and conductivity detection. Elution solvent was 8 mmol·L^{−1} sodium carbonate (Fisher Scientific, Illkirch, France) in ultrapure water. A Metrosep A Supp 5250/4.0 column with an adequate precolumn at a temperature of 35 °C was used. The calibration curve was linear in the range from 0.06 to 2000 μmol·kg^{−1} ($R^2 = 0.999$).

Preparation of Pickering Emulsions and Characterization. Nitrobenzene NB (C₆H₅NO₂, 95%, Aldrich; solubility in water, 0.19 wt % at 20 °C) constituted the oil phase of the Pickering emulsions. In the beginning, aqueous dispersions of 1 wt % TiO₂ or TiO₂-F were obtained by means of an UltraTurrax T25 rotor-stator device equipped with a S25N18G shaft (IKA, Germany) rotating at 22000 rpm for 5 min to de-aggregate the particles. Thereafter, NB (up to 20

vol %) was added to the aqueous dispersion and stirred during 5 min with an UltraTurrax T25 under the same conditions. The size distribution of the TiO₂ nanoparticles was determined by dynamic light scattering using a Zetasizer NanoZS instrument (Malvern, U.K.).

Emulsions droplets were observed by optical microscopy using a Leica DMLM (Germany) microscope equipped with a video camera. The concentrated emulsions were diluted and spread between a glass plate and cover slip for microscopic observation in transmission mode and image analysis. The size distribution was determined using analysis image software AnalySIS.

Droplet size measurements of O/W emulsions were carried out at small-angle light scattering using a Mastersizer 3000 instrument (Malvern, U.K.). The refractive indexes of the optical model used for data processing were 1.332 for water and 1.552 for NB.

The electrical conductivity of emulsions was measured with a Radiometer CDM 210 conductivity meter at 25 °C.

Contact angles of NB/photocatalyst/water were measured by the sessile drop method on the flat photocatalyst surface using the Drop Shape Analysis System DSA10Mk2 (Krüss, Germany). A pellet of the photocatalyst was pressed under 7 kPa pressure. A drop of NB (volume, 5–6 μL) was deposited on the surface of the pellet immersed in water with a syringe needle and the drop picture was recorded with a CCD camera.

Photocatalytic Experiments. The photocatalytic experiments were carried out in a cylindrical Pyrex batch photoreactor (diameter: 10 cm) equipped with a mechanical stirrer rotating at 500 rpm. Emulsion (160 mL) containing 0.1 vol % NB and 1 wt % catalyst was illuminated by a PLL lamp UVA (8 mW·cm⁻²) placed horizontally below the photoreactor. The lateral walls were covered with aluminum foil. Cooling water circulated in a thimble surrounding the reactor to maintain the temperature at an ambient value. Samples were withdrawn at fixed time intervals, mixed with 50 vol % acetonitrile/water (50/50) solution to break the emulsion trapped by solid particles, and filtered (Millipore, PTFE, 0.45 μm) before analysis.

Notably, the amount of catalyst chosen for the photodegradation tests was selected from a compromise between issues related to photocatalysis and to the stability of the emulsion. The amount of photocatalyst allowed one to neglect the backscattering, which would be relevant only for small values of the optical thickness.⁵³ Nevertheless, as the system was not optimized with respect to the radiant field distribution, no information on the intrinsic reaction kinetics could be retrieved. Therefore, the apparent kinetic constants reported throughout the text are intended to provide only a numerical comparison between degradation kinetics obtained under the same experimental conditions.

The time evolution of the photocatalytic degradation of NB emulsion was followed by using a HPLC system model 1290 Infinity. This apparatus was equipped with a binary pump (Agilent Technologies, G4220B), autosampler (Agilent Technologies, 1290 Sampler), photodiode array (PDA) detector (Agilent Technologies, 1260), and C18 NUCLEOSIL 100-5 column (Machery Nagel: 4.6 × 250 mm). The injected sample volume was 20 μL. The eluent circulating at a flow rate of 1 mL·min⁻¹ consisted of ultrapure water (40%) and acetonitrile (60%). The resulting data were collected by using Agilent Mass Hunter software.

RESULTS AND DISCUSSION

Emulsification Experiments. The formulation process of Pickering emulsions requires a precise control of the intervening parameters to effectively tailor type, stability, and droplet size. Preliminary experiments aimed to show the feasibility of the formulation of nitrobenzene/water (NB/W) emulsions with pristine TiO₂ and TiO₂-F as the stabilizers.

Figure 1A,B presents NB/W emulsions obtained in the presence of pristine TiO₂ and TiO₂-F, respectively. In both cases, the phase containing NB sedimented, leaving a

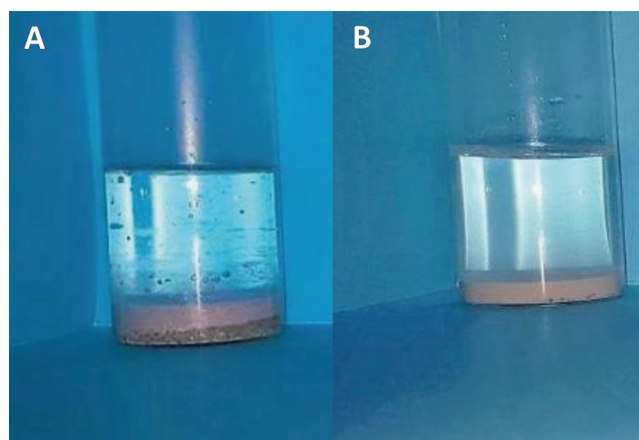


Figure 1. NB (20 vol %)/water Pickering emulsions stabilized by 1 wt % pristine TiO₂ (A) and TiO₂-F (B). Both pictures taken after 24 h storage at rest show a clear aqueous supernatant because all materials denser than water underwent sedimentation. Panel (A) shows sediment of solid particles of TiO₂ that are not adsorbed at the NB–water interface topped by a layer of mixed pure NB and coarse emulsion. Panel (B) shows sediment of Pickering emulsion and no free TiO₂-F particles.

supernatant aqueous phase due to the higher density of NB (1.2 g·mL⁻¹) with respect to water.

When pristine TiO₂ was used as the emulsifier (Figure 1A), fast sedimentation of TiO₂ particles took place and a release of NB was observed. Therefore, pristine TiO₂ nanoparticles were unable to stabilize the NB/W emulsions. In fact, the hydrophobic NB molecules show low tendency to adsorb onto the hydroxylated and highly hydrophilic TiO₂ surface. Conversely, TiO₂-F could stabilize NB/W emulsions quite efficiently under the same conditions (Figure 1B). The droplet size was ca. 128 μm and no release of pure NB was observed during at least 2 months (Figure 2). The NB droplets undergo sedimentation quite fast because of the density of NB higher than water and quite large droplet size. The mean diameter of the NB droplets, however, did not change during storage, demonstrating that coalescence did not occur.

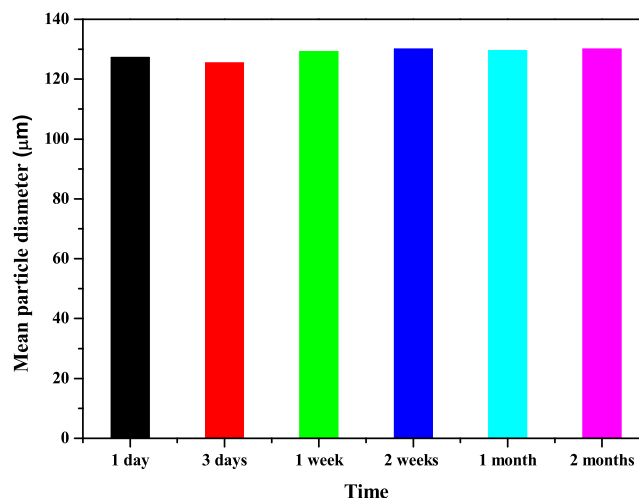


Figure 2. Mean droplet size of NB (20 vol %) in Pickering emulsions stabilized by 1 wt % TiO₂-F nanoparticles as a function of time. *T* = 25 °C. Each measurement was repeated three times and the standard deviation was lower than ±4%.

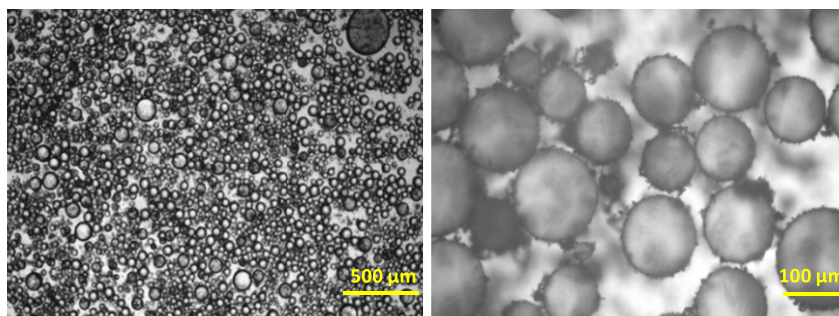
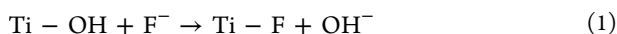


Figure 3. Optical microscopy images of NB (20 vol %) in water emulsions stabilized by TiO₂-F (1 wt %).

These results were confirmed by the optical microscopy images shown in Figure 3 where it is evident that NB droplets of ca. 130 μm in size are nicely dispersed in a continuous water phase.

The different behavior of the TiO₂-F sample with respect to the pristine TiO₂ material can be explained by its surface properties. The fluorinated material was prepared by a simple ligand exchange of surface hydroxyl groups with F⁻ ions,^{54,55} as expressed by eq 1.



Equation 1 does not express a simple adsorption equilibrium of F⁻ ions because fluoride modification is stable upon washing during the preparation procedure and reverse process, a nucleophilic substitution by hydroxide ions, requires high NaOH concentrations (ca. 1 M), and does not reach completion.⁵⁶

The surface density of F⁻ ions on the surface of TiO₂ has been determined by means of ion chromatography. By considering that the specific surface area of the TiO₂ sample is 103 m²·g⁻¹ and its average hydroxylation degree ranges between 4.8 and 6.1 Ti-OH·nm⁻²,⁵⁷ a maximum fluorine grafting was achieved at pH = 3.2. The fluorine surface density was 3 fluorinated surface sites per nm², corresponding to 50–60% of the total surface sites.⁵⁰ Therefore, the surface of the fluorinated TiO₂ presents two functionalities almost equally distributed, which endow it with amphiphilic features.

Contact Angle Measurements. The stabilization of Pickering emulsions requires that partial wetting condition of the solid particles by water and NB is fulfilled. The wettability of the photocatalyst was assessed by means of contact angle measurements. The classical technique of contact angle measurement consists of the optical observation of a small drop of oil deposited onto the solid surface immersed in water (or of a drop of water deposited on the surface immersed in oil) and the determination of the contact angle in water on the picture. Furthermore, this technique affords information on the type and stability of Pickering emulsions.^{18,58} In particular, contact angles close to 90° provide the most efficient stabilization of Pickering emulsions. Contact angles lower than 90° are indicative of hydrophilic particles that can better stabilize oil-in-water emulsions, while particles with contact angles higher than 90° better stabilize water-in-oil emulsions.

It was not possible to calculate the contact angle of NB over pristine TiO₂ because the drop of NB floated and rolled on the surface of the solid. This indicated total wetting by water and the absence of any interaction between TiO₂ and NB. This result explains why it was not possible to stabilize Pickering emulsions containing NB by using pristine TiO₂ as

the emulsifier. On the contrary, the measurement was possible on the TiO₂-F sample as shown in Figure 4.

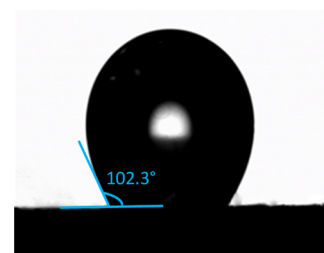


Figure 4. Drop of NB on the TiO₂-F surface immersed in water. $T = 25^\circ\text{C}$.

A drop of NB on TiO₂-F immersed in water presents a contact angle of $102.3 \pm 0.6^\circ$. This indicates partial wettability and lower hydrophilicity of the TiO₂-F surface with respect to the pristine TiO₂. Such a contact angle close to 90° allows the stabilization of either O/W or W/O Pickering emulsions by TiO₂-F particles, depending on the relative amounts of oil and water.⁵⁹ Hence, NB/water emulsions should be obtained when the NB content is smaller than that of water.

Characterization of the Emulsion. Two crucial features of the emulsion have been investigated: the size of the droplets and the type of emulsion as a function of the amount of the solid nanoparticles (TiO₂-F) and of the volume fraction of the oil phase (Φ_{NB}).

The type of emulsion has been identified by varying the volume fraction of NB (Figure 5A). Conductivity measurements performed on emulsions with different volume fractions of the oil phase gave evidence of a phase inversion phenomenon from O/W type (NB droplets in water, high conductivity) to W/O type (water droplets in NB, low conductivity) when Φ_{NB} exceeded ca. 50 vol %. Notably, the possibility to switch between two emulsion types is a significant advantage of the present system with respect to analogous systems stabilized by surfactants; therefore, it is possible to stabilize with the same type of particle both direct and inverse emulsions.

The droplet size is a relevant parameter characterizing the ability of adsorbed particles to stabilize the emulsion. The stability of Pickering emulsions is governed by the reduction of the free energy of the system caused by the transfer of the photocatalyst from the aqueous dispersion to the NB/W interface. This transfer produces a variation in the size of the droplets and the consequent increase in the interfacial area. Therefore, the droplet size mainly depends on the amount of stabilizer (TiO₂-F). Figure 5B shows the changes in the mean

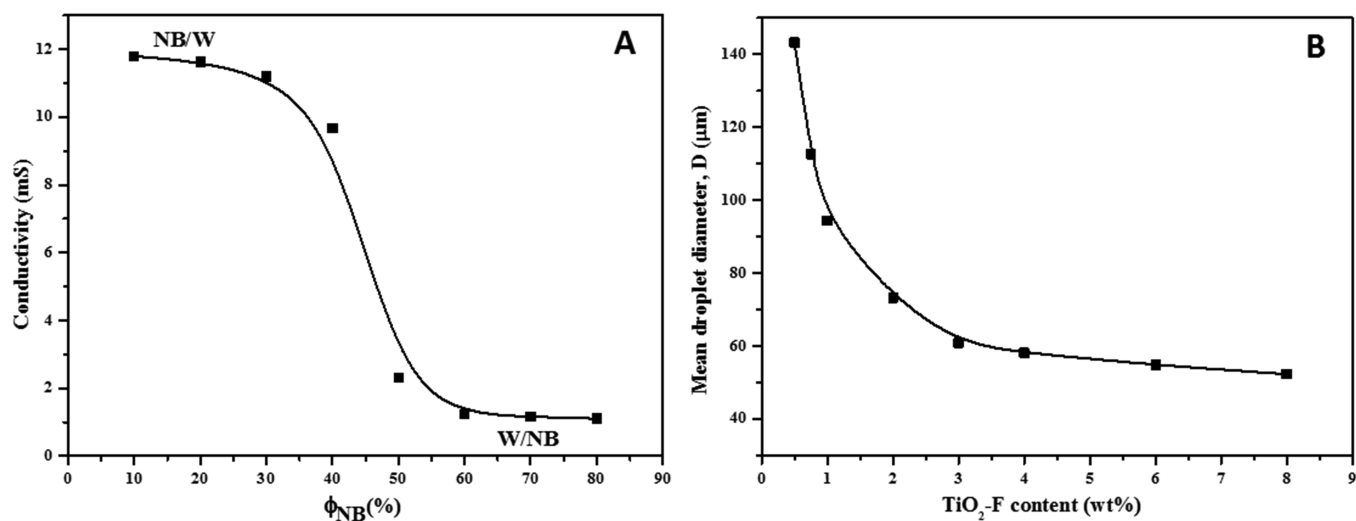


Figure 5. (A) Phase inversion of emulsions of NB in water stabilized by $\text{TiO}_2\text{-F}$ (1 wt %) nanoparticles. (B) Mean NB droplet diameter of NB (20 vol %)/water emulsions as a function of $\text{TiO}_2\text{-F}$ content. $T = 25^\circ\text{C}$.

diameter of the droplets at different contents of $\text{TiO}_2\text{-F}$ while keeping the amount of NB constant (20 vol %). At low concentration of $\text{TiO}_2\text{-F}$ (less than 0.5 wt %), emulsions were not stable and coalesced immediately after the emulsification procedure. Conversely, the stability of Pickering emulsions increased for $\text{TiO}_2\text{-F}$ loadings higher than 0.5 wt %. By increasing the content of $\text{TiO}_2\text{-F}$ nanoparticles, the droplet size decreased until it reached a “plateau”, where further increasing the $\text{TiO}_2\text{-F}$ content did not result in size reduction. Indeed, $\text{TiO}_2\text{-F}$ concentrations above 4 wt % produced almost a constant NB droplet size (mean value, 57.5 μm). This can be explained by a lack of efficiency of the emulsification process because the UltraTurrax disperser was unable to reduce the NB droplet size down to the sizes that would have been expected by extrapolation of the curve in the first regime. As a consequence, $\text{TiO}_2\text{-F}$ nanoparticles were in excess once the plateau region was reached.

In the plateau region, the Pickering emulsion is comprised of micrometer-sized NB droplets surrounded by $\text{TiO}_2\text{-F}$, which dually acts as a stabilizer and, once irradiated, as a photocatalyst. Therefore, the stabilized droplets can be seen as microreactors in which the photocatalytic reaction rate can be maximized due to the reduced mass transfer limitations and to the enhanced contact area between the substrate and photocatalyst.

Photocatalytic Activity. The photocatalytic experiments were performed using NB/water/ $\text{TiO}_2\text{-F}$ Pickering emulsions containing 0.1 vol % NB (1200 ppm). Figure 6 shows the mean size distribution of the NB droplets along with an optical microscopy image (inset) of the emulsion.

A stable Pickering emulsion with small NB droplets nicely dispersed in water is evident. Most of the droplets have a diameter ranging between 1.5 and 3 μm , while a smaller fraction presents diameters ranging between 0.3 and 0.6 μm . This smaller fraction corresponds to the amount of $\text{TiO}_2\text{-F}$ in excess that was not adsorbed on the surface of the NB droplets.

The presence of fluorine dually acts in improving the photocatalytic system. In fact, it enhances the photocatalytic activity with respect to pristine TiO_2 and stabilizes the emulsion, favoring the formation of micrometer-sized droplets.

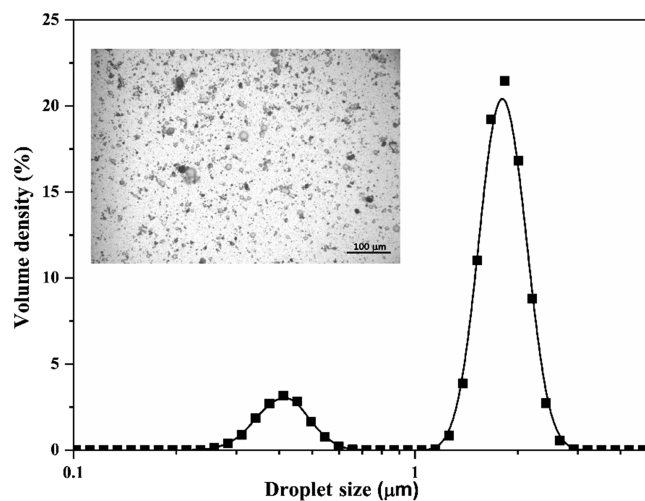


Figure 6. Mean size distribution of the NB droplets. Inset: Optical microscopy image of the emulsion ([NB]: 0.1 vol %; $\text{TiO}_2\text{-F}$ amount: 1 wt %). $T = 25^\circ\text{C}$.

The superior photocatalytic activity of the fluorinated TiO_2 has been tested by choosing an initial NB concentration, which could dissolve in water, i.e., 50 ppm, and performing its photodegradation in the presence of TiO_2 and $\text{TiO}_2\text{-F}$. Results are reported in Figure 7.

The NB photodegradation is faster in the presence of the fluorinated sample. In particular, the apparent observed kinetic constants, determined by differentiating the experimental data at the initial time, by using a five-point formula for equally spaced points,^{60,61} were 16×10^{-3} and $12 \times 10^{-3} \text{ min}^{-1}$ for the fluorinated and bare samples, respectively. This evidence, often reported in the literature, has been generally related to the higher availability of photogenerated holes, which eventually results in higher production of hydroxyl radicals.⁴³ Other authors attributed the enhanced activity to the presence of singlet oxygen generated through a prevailing energy transfer mechanism.⁴⁴ Moreover, the intraband-gap energy states within 1.3 eV above the valence band, whose existence has been theoretically predicted^{62,63} and only recently experimentally demonstrated,⁵⁰ could also be beneficial, acting as traps, enhancing the life time of the photogenerated holes.

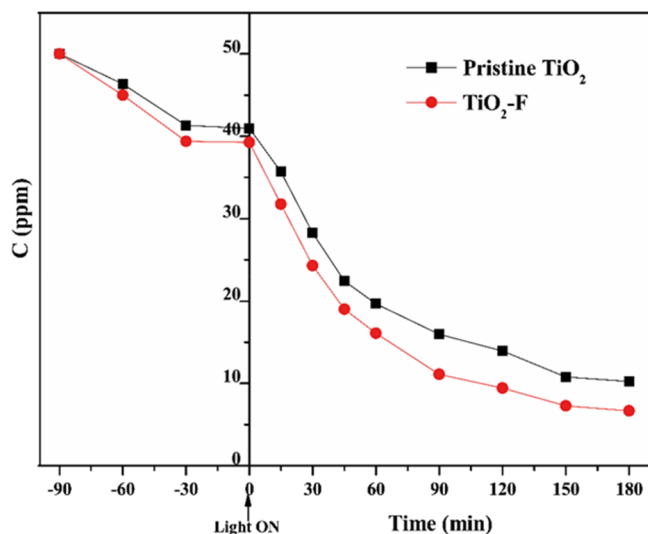


Figure 7. Photodegradation of NB aqueous solutions over pristine TiO_2 and $\text{TiO}_2\text{-F}$ under UV irradiation. Initial concentration of NB was 50 ppm. The sample was in the dark at negative times before the UV light was switched on. $T = 25\text{ }^\circ\text{C}$.

However, by taking into account the above reported surface features, the affinity of the photocatalyst surface with the organic substrate may also play a significant role. In fact, TiO_2 surface fluorination decreases its hydrophilicity, favoring the adsorption of NB and then its direct oxidation through the photogenerated holes.

To provide evidence of the contribution of the emulsification process on the photocatalytic activity, the photodegradation of NB has been carried out in emulsified and nonemulsified NB/water mixtures in the presence of $\text{TiO}_2\text{-F}$. The results of the runs are illustrated in Figure 8 in terms of normalized concentration (NB concentration at time t /initial NB concentration $\times 100$). For the sake of comparison, an experiment in the absence of the photocatalyst is also reported.

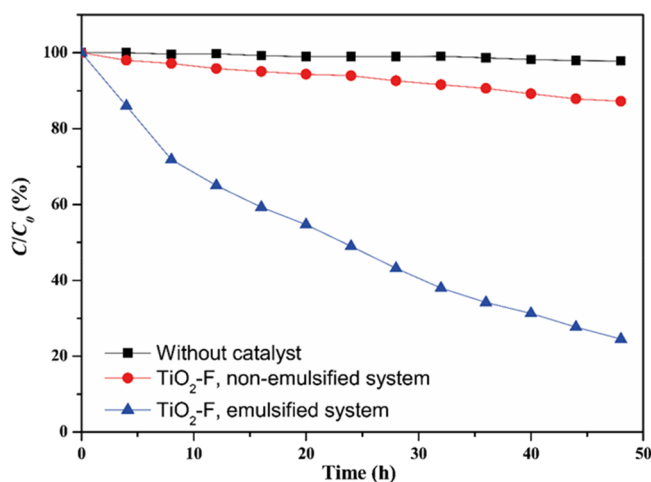


Figure 8. Normalized NB concentration (C/C_0) during irradiation time in the absence of photocatalyst (black squares), in the presence of $\text{TiO}_2\text{-F}$ but without emulsification (red circles), and in the presence of $\text{TiO}_2\text{-F}$ after emulsification (blue triangles). Photocatalyst amount: 1 wt %; initial NB concentration: 0.1 vol % (1200 ppm). $T = 25\text{ }^\circ\text{C}$.

NB concentration always decreased in the presence of $\text{TiO}_2\text{-F}$ photocatalyst under UV irradiation. However, only 13% of the initial NB concentration was photodegraded after 48 h in the case of the nonemulsified NB/W system. The photocatalytic degradation was significantly higher in the emulsified systems, reaching 75% after the same reaction time. The apparent rate constants, determined as above, were 0.7×10^{-3} and $0.04 \times 10^{-3}\text{ min}^{-1}$ for the emulsified and nonemulsified $\text{TiO}_2\text{-F}$ systems, respectively. In other words, the emulsified system showed an initial NB degradation rate ca. 18 times greater than that retrieved for the nonemulsified system.

By comparing the results reported in Figures 7 and 8, it is evident that the stabilizing effect of $\text{TiO}_2\text{-F}$ plays a predominant role in determining the global efficiency with respect to the intrinsic higher efficiency of the fluorinated sample. In fact, the amphiphilic properties of the fluorinated surface give rise to adsorption equilibrium of the two phases, thus increasing the dispersive capacity of the $\text{TiO}_2\text{-F}$ nanoparticles and thermodynamically favoring the formation of micrometer-sized NB droplets. The resulting high contact surface area between the photocatalyst and substrate improves the photocatalytic activity. Indeed, by considering the photoreactor volume $V = 160\text{ mL}$, volume fraction of NB $\Phi_{\text{NB}} = 0.1\text{ vol } \%$, and NB droplet size $D = 2\text{ }\mu\text{m}$, the total NB–water interfacial area in the emulsified system is 0.48 m^2 as calculated by eq 2.

$$A = \frac{6V\Phi_{\text{NB}}}{D} = 0.48\text{ m}^2 \quad (2)$$

Contrarily, in the nonemulsified system, the photocatalyst nanoparticles are mainly located at the planar interface between the two liquid phases (ca. $8 \times 10^{-3}\text{ m}^2$).

Notably, by considering that only half of the surface hydroxyl groups are substituted by fluorine, adsorption of water still takes place, contributing to the photocatalytic reaction in various ways. Photogenerated holes induce water oxidation and produce hydroxyl radicals, which can in turn oxidize NB. Moreover, water may compete for adsorption with oxygenated degradation products, thus avoiding poisoning of the photocatalyst. It is worth mentioning that even if the apparent rate constant of $\text{TiO}_2\text{-F}$ in emulsion ($0.7 \times 10^{-3}\text{ min}^{-1}$) is much smaller than that in solution ($16 \times 10^{-3}\text{ min}^{-1}$), in the first case, it was possible to treat 1200 ppm NB, while only 50 ppm could be treated in solution. At this high NB concentration, the “classical” nonemulsified $\text{TiO}_2\text{-F}$ system is virtually not active ($0.04 \times 10^{-3}\text{ min}^{-1}$). Therefore, the size distribution of the droplets is a critical parameter both for the photocatalytic activity and for the stability of the emulsion. The remarkable efficiency enhancement observed in the emulsified system allows one to treat in one-pot high amounts of insoluble pollutants without implementing physical separation methods, which, in any case, require costly chemical degradation downstream.

The oxidation by products of the photocatalytic oxidation of NB dissolved in TiO_2 aqueous suspensions has been already reported in the relevant literature as mainly derived from NB hydroxylation induced by hydroxyl radicals photocatalytically generated.^{3,6,64} Accordingly, in the present investigation, 4-nitrophenol (4-NP) and 3-nitrophenol (3-NP) were the main intermediates after 180 min irradiation time for the NB degradation tests shown in Figure 7. Figure 9 reports the correspondent chromatograms and UV–vis spec-

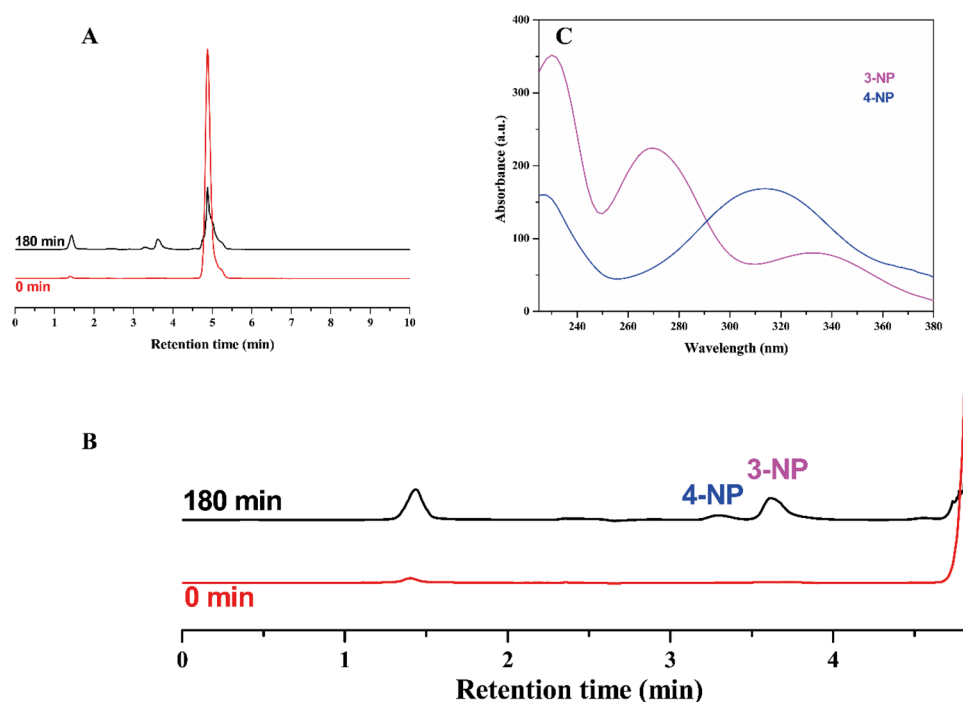


Figure 9. (A) Chromatograms of samples collected at the start and after 180 min irradiation time for the NB degradation test in the presence of $\text{TiO}_2\text{-F}$, as shown in Figure 7 (initial NB concentration: 50 ppm). (B) Zoom of the chromatograms highlighting the two oxidation by-products identified as 4-nitrophenol (4-NP) and 3-nitrophenol (3-NP), whose UV-vis spectra are shown in (C). The peak at 1.4 min marks the dead volume of the column.

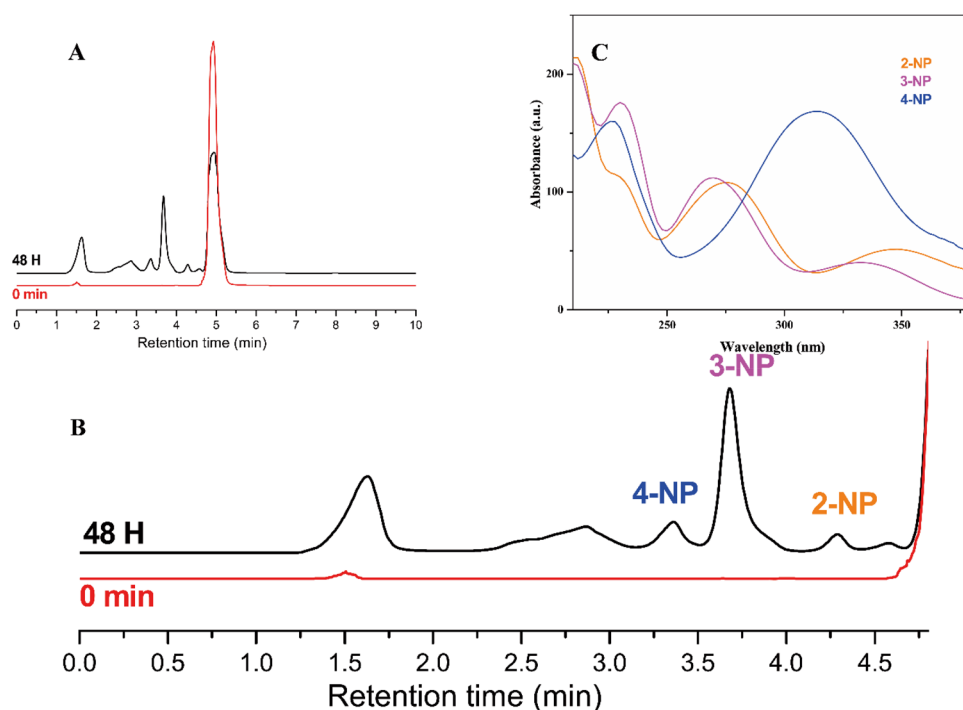


Figure 10. (A) Chromatograms of samples collected at the start and after 48 h irradiation time for the NB degradation test in NB/W emulsion in the presence of $\text{TiO}_2\text{-F}$, as shown in Figure 8 (initial NB concentration: 1200 ppm). (B) Zoom of the chromatograms highlighting the three oxidation by-products identified as 4-nitrophenol (4-NP), 3-nitrophenol (3-NP), and 2-nitrophenol (2-NP), whose UV-vis spectra are shown in (C). The peak at 1.5 min marks the dead volume of the column.

tra of the intermediates for the run carried out in the presence of $\text{TiO}_2\text{-F}$.

The intermediates were the same also in the presence of TiO_2 (data not shown), indicating, as expected, that in both

cases, the hydroxyl radical attack triggers NB degradation. Notably, 3-NP is the most abundant intermediate according to the activating, meta orienting nature of the nitro substituent.

Performing the reaction in NB/W emulsion (as in the runs shown in Figure 8) did not significantly affect the degradation mechanism. Figure 10 shows the intermediates identified after 48 h irradiation in the TiO₂-F stabilized emulsion, along with their UV–vis spectra.

Small amounts of 2-NP have been detected along with the 4-NP and 3-NP isomers, with the latter being the most abundant as mentioned above. A small and broad peak is detectable between 2.25 and 3.25 min, which could not be identified due to the low intensity and probable overlapping of signals related to different species. However, it is plausible to ascribe this signal to di-hydroxylated compounds such as nitrocatechol or nitroresorcinol, which are more hydrophilic compounds than the nitrophenol isomers, and consequently have lower retention time. This is also in agreement with Bhatkhande et al.,⁶ which also detected these intermediates in smaller amounts with respect to the monohydroxylated products.

CONCLUSIONS

The present paper reports the possibility of exploiting the unique amphiphilic properties of the fluorinated surface of TiO₂ to stabilize Pickering emulsions of organic pollutants poorly soluble in water. The obtained system is comprised of small droplets of substrate surrounded by the photocatalyst that act as microreactors for the degradation of the pollutant. This configuration allows obtaining 18 times faster photodegradation with respect to the nonemulsified system. The characterization of the physicochemical properties of the emulsion shows an inversion of the type of emulsion (from oil in water to water in oil) obtained by changing the amount of organic phase in the system. Moreover, the stabilizing ability of the fluorinated TiO₂ nanoparticles due to their amphiphilic surface is highlighted. Therefore, the role of fluorination is dual. On one hand, fluorination affects both the electronic and surface properties of TiO₂ and enhances the photocatalytic activity due to the higher production of hydroxyl radicals. On the other hand, the peculiar surface features allow one to stabilize NB emulsions, which was not possible by using bare TiO₂. The present results shed some light on the hydrophilicity of the fluorinated surface of TiO₂ and open the route for one-pot treatments of biphasic polluted streams without the need of preliminary physical separation.

AUTHOR INFORMATION

Corresponding Authors

Yves Chevalier – *University of Lyon, Laboratoire d'Automatique et de Génie des Procédés (LAGEPP), UMR 5007 CNRS, University Claude Bernard Lyon 1, 69622 Villeurbanne, France;* orcid.org/0000-0002-7526-5658; Email: yves.chevalier@univ-lyon1.fr

Francesco Parrino – *Department of Industrial Engineering, University of Trento, 38123 Trento, Italy;* orcid.org/0000-0001-7507-941X; Email: francesco.parrino@unitn.it

Authors

Nidhal Fessi – *Laboratoire de Recherche Catalyse et Matériaux pour l'Environnement et les Procédés LRCMEP (UR11ES85), Faculté des Sciences de Gabès, University of Gabès, 6072 Gabès, Tunisia; University of Lyon, Laboratoire d'Automatique et de Génie des Procédés (LAGEPP), UMR 5007 CNRS, University Claude Bernard Lyon 1, 69622 Villeurbanne, France*

Mohamed Faouzi Nsib – *Laboratoire de Recherche Catalyse et Matériaux pour l'Environnement et les Procédés LRCMEP (UR11ES85), Faculté des Sciences de Gabès, University of Gabès, 6072 Gabès, Tunisia; Higher School of Sciences and Technology, University of Sousse, 4003 Sousse, Tunisia*

Chantal Guillard – *University of Lyon, Institut de Recherches sur la Catalyse et l'Environnement de Lyon (IRCELYON), UMR 5256 CNRS, Université Claude Bernard Lyon 1, 69626 Villeurbanne, France*

Frédéric Dappozze – *University of Lyon, Institut de Recherches sur la Catalyse et l'Environnement de Lyon (IRCELYON), UMR 5256 CNRS, Université Claude Bernard Lyon 1, 69626 Villeurbanne, France*

Ammar Houas – *Laboratoire de Recherche Catalyse et Matériaux pour l'Environnement et les Procédés LRCMEP (UR11ES85), Faculté des Sciences de Gabès, University of Gabès, 6072 Gabès, Tunisia*

Leonardo Palmisano – *Dipartimento di Ingegneria, University of Palermo, 90128 Palermo, Italy;* orcid.org/0000-0002-3951-2260

Complete contact information is available at:

<https://pubs.acs.org/10.1021/acs.langmuir.0c02285>

Notes

The authors declare no competing financial interest.

REFERENCES

- (1) Zhang, T.; Ma, J. Catalytic Ozonation of Trace Nitrobenzene in Water with Synthetic Goethite. *J. Mol. Catal. A: Chem.* **2008**, *279*, 82–89.
- (2) Guy, R. C. Nitrobenzene. In *Encyclopedia of Toxicology*; Second Edition; Academic Press: 2005, 236–238.
- (3) Palmisano, G.; Loddo, V.; Augugliaro, V.; Palmisano, L.; Yurdakal, S. Photocatalytic Oxidation of Nitrobenzene and Phenylamine: Pathways and Kinetics. *AIChE J.* **2007**, *53*, 961–968.
- (4) Majumder, P. S.; Gupta, S. K. Hybrid Reactor for Priority Pollutant Nitrobenzene Removal. *Water Res.* **2003**, *37*, 4331–4336.
- (5) Jo, W.-K.; Won, Y.; Hwang, I.; Tayade, R. J. Enhanced Photocatalytic Degradation of Aqueous Nitrobenzene Using Graphitic Carbon–TiO₂ Composites. *Ind. Eng. Chem. Res.* **2014**, *53*, 3455–3461.
- (6) Bhatkhande, D. S.; Pangarkar, V. G.; Beenackers, A. A. C. M. Photocatalytic Degradation of Nitrobenzene Using Titanium Dioxide and Concentrated Solar Radiation: Chemical Effects and Scale up. *Water Res.* **2003**, *37*, 1223–1230.
- (7) Latifoglu, A.; Gurol, M. D. The Effect of Humic Acids on Nitrobenzene Oxidation by Ozonation and O₃/UV Processes. *Water Res.* **2003**, *37*, 1879–1889.
- (8) Tada, H.; Ishida, T.; Takao, A.; Ito, S. Drastic Enhancement of TiO₂-Photocatalyzed Reduction of Nitrobenzene by Loading Ag Clusters. *Langmuir* **2004**, *20*, 7898–7900.
- (9) Zhao, L.; Ma, J.; Sun, Z. Z. Oxidation Products and Pathway of Ceramic Honeycomb-Catalyzed Ozonation for the Degradation of Nitrobenzene in Aqueous Solution. *Appl. Catal. B* **2008**, *79*, 244–253.
- (10) Zhang, S. J.; Jiang, H.; Li, M. J.; Yu, H. Q.; Yin, H.; Li, Q. R. Kinetics and Mechanisms of Radiolytic Degradation of Nitrobenzene in Aqueous Solutions. *Environ. Sci. Technol.* **2007**, *41*, 1977–1982.
- (11) International Maritime Organization (IMO). *2008 revised guidelines for systems for handling oily wastes in machinery spaces of ships incorporating guidance notes for an integrated bilge water treatment system*; IMO: 2008.
- (12) Cataldo, S.; Ianni, A.; Loddo, V.; Mirenda, E.; Palmisano, L.; Parrino, F.; Piazzese, D. Combination of advanced oxidation processes and active carbons adsorption for the treatment of simulated saline wastewater. *Sep. Purif. Technol.* **2016**, *171*, 101–111.

- (13) Parrino, F.; Camera-Roda, G.; Loddo, V.; Augugliaro, V.; Palmisano, L. Maximization of the Reaction Rate and Control of Undesired By-Products. *Appl. Catal. B* **2015**, *178*, 37–43.
- (14) Bellardita, M.; Loddo, V.; Mele, A.; Panzeri, W.; Parrino, F.; Pibiri, I.; Palmisano, L. Photocatalysis in Dimethyl Carbonate Green Solvent: Degradation and Partial Oxidation of Phenanthrene on Supported TiO₂. *RSC Adv.* **2014**, *4*, 40859–40864.
- (15) Cambié, D.; Bottecchia, C.; Straathof, N. J. W.; Hessel, V.; Noël, T. Applications of Continuous-Flow Photochemistry in Organic Synthesis, Material Science, and Water Treatment. *Chem. Rev.* **2016**, *116*, 10276–10341.
- (16) Pickering, S. U. Emulsions. *J. Chem. Soc.* **1907**, *91*, 2001–2021.
- (17) Aveyard, R.; Binks, B. P.; Clint, J. H. Emulsions Stabilized Solely by Solid Colloidal Particles. *Adv. Colloid Interface Sci.* **2003**, *100–102*, 503–546.
- (18) Binks, B. P. Particles as Surfactants—Similarities and Differences. *Curr. Opin. Colloid Interface Sci.* **2002**, *7*, 21–41.
- (19) Binks, B. P.; Horozov, T. S. *Colloidal Particles at Liquid Interfaces*; Cambridge University Press: 2006.
- (20) Chevalier, Y.; Bolzinger, M.-A. Emulsions Stabilized with Solid Nanoparticles: Pickering Emulsions. *Colloids Surf. A* **2013**, *439*, 23–34.
- (21) Menon, V. B.; Wasan, D. T. Coalescence of Water-in-Shale Oil Emulsions. *Sep. Sci. Technol.* **1984**, *19*, 555–574.
- (22) Eley, D. D.; Hey, M. J.; Lee, M. A. Rheological Studies of Asphaltene Films Adsorbed at the Oil/Water Interface. *Colloids Surf.* **1987**, *24*, 173–182.
- (23) Eley, D. D.; Hey, M. J.; Symonds, J. D. Emulsions of Water in Asphaltene-Containing Oils. 1. Droplet Size Distribution and Emulsification. *Colloids Surf.* **1988**, *32*, 87–101.
- (24) Yang, F.; Liu, S.; Xu, J.; Lan, Q.; Wei, F.; Sun, D. Pickering Emulsions Stabilized Solely by Layered Double Hydroxides Particles: The Effect of Salt on Emulsion Formation and Stability. *J. Colloid Interface Sci.* **2006**, *302*, 59–169.
- (25) Marku, D.; Wahlgren, M.; Rayner, M.; Sjö, M.; Timgren, A. Characterization of Starch Pickering Emulsions for Potential Applications in Topical Formulations. *Int. J. Pharm.* **2012**, *428*, 1–7.
- (26) Chen, H.; Zhu, H.; Hu, J.; Zhao, Y.; Wang, Q.; Wan, J.; Yang, Y.; Xu, H.; Yang, X. Highly Compressed Assembly of Deformable Nanogels into Nanoscale Suprastructures and Their Application in Nanomedicine. *ACS Nano* **2011**, *5*, 2671–2680.
- (27) Frelichowska, J.; Bolzinger, M.-A.; Pelletier, J.; Valour, J.-P.; Chevalier, Y. Topical Delivery of Lipophilic Drugs from o/w Pickering Emulsions. *Int. J. Pharm.* **2009**, *371*, 56–63.
- (28) Dickinson, E. Food Emulsions and Foams: Stabilization by Particles. *Curr. Opin. Colloid Interface Sci.* **2010**, *15*, 40–49.
- (29) Rayner, M.; Timgren, A.; Sjö, M.; Dejmek, P. Quinoa Starch Granules: A Candidate for Stabilising Food-Grade Pickering Emulsions. *J. Sci. Food Agric.* **2012**, *92*, 1841–1847.
- (30) Crossley, S.; Faria, J.; Shen, M.; Resasco, D. E. Solid Nanoparticles that Catalyze Biofuel Upgrade Reactions at the Water/Oil Interface. *Science* **2010**, *327*, 68–72.
- (31) Leclercq, L.; Mouret, A.; Proust, A.; Schmitt, V.; Bauduin, P.; Aubry, J.-M.; Nardello-Rataj, V. Pickering Emulsion Stabilized by Catalytic Polyoxometalate Nanoparticles: A New Effective Medium for Oxidation Reactions. *Chem. – Eur. J.* **2012**, *18*, 14352–14358.
- (32) Holdich, R. G.; Ipek, I. Y.; Lazrigh, M.; Shama, G. Production and Evaluation of Floating Photocatalytic Composite Particles Formed Using Pickering Emulsions and Membrane Emulsification. *Ind. Eng. Chem. Res.* **2012**, *51*, 12509–12516.
- (33) Yang, H.; Fu, L.; Wei, L.; Liang, J.; Binks, B. P. Compartmentalization of Incompatible Reagents within Pickering Emulsion Droplets for One-pot Cascade Reactions. *J. Am. Chem. Soc.* **2015**, *137*, 1362–1371.
- (34) Leclercq, L.; Mouret, A.; Renaudineau, S.; Schmitt, V.; Proust, A.; Nardello-Rataj, V. Self-assembled Polyoxometalates Nanoparticles as Pickering Emulsion Stabilizers. *J. Phys. Chem. B* **2015**, *119*, 6326–6337.
- (35) Chen, Z.; Zhao, C.; Ju, E.; Ji, H.; Ren, J.; Binks, B. P.; Qu, X. Design of Surface-active Artificial Enzyme Particles to Stabilize Pickering emulsions for High-performance Biphasic Biocatalysis. *Adv. Mater.* **2016**, *28*, 1682–1688.
- (36) Yang, B.; Leclercq, L.; Clacens, J.-M.; Nardello-Rataj, V. Acidic/amphiphilic Silica Nanoparticles: New Eco-friendly Pickering Interfacial Catalysis for Biodiesel Production. *Green Chem.* **2017**, *19*, 4552–4562.
- (37) Cakmak, F. P.; Keating, C. D. Combining Catalytic Microparticles with Droplets Formed by Phase Coexistence: Adsorption and Activity of Natural Clays at the Aqueous/aqueous Interface. *Sci. Rep.* **2017**, *7*, 3215.
- (38) Pera-Titus, M.; Leclercq, L.; Clacens, J.-M.; De Campo, F.; Nardello-Rataj, V. Pickering Interfacial Catalysis for Biphasic Systems: From Emulsion Design to Green Reactions. *Angew. Chem., Int. Ed.* **2015**, *54*, 2006–2021.
- (39) Fessi, N.; Nsib, M. F.; Chevalier, Y.; Guillard, C.; Dapozze, F.; Houas, A.; Palmisano, L.; Parrino, F. Photocatalytic Degradation Enhancement in Pickering Emulsions Stabilized by Solid Particles of Bare TiO₂. *Langmuir* **2019**, *35*, 2129–2136.
- (40) Nawaz, M.; Miran, W.; Jang, J.; Lee, D. S. Stabilization of Pickering Emulsion with Surface-modified Titanium Dioxide for Enhanced Photocatalytic Degradation of Direct Red 80. *Catal. Today* **2017**, *282*, 38–47.
- (41) Nsib, M. F.; Maayoufi, A.; Moussa, N.; Tarhouni, N.; Massouri, A.; Houas, A.; Chevalier, Y. TiO₂ Modified by Salicylic Acid as a Photocatalyst for the Degradation of Monochlorobenzene via Pickering Emulsion way. *J. Photochem. Photobiol., A* **2013**, *251*, 10–17.
- (42) Dozzi, M. V.; D’Andrea, C.; Ohtani, B.; Valentini, G.; Selli, E. Fluorine-Doped TiO₂ Materials: Photocatalytic Activity vs Time-Resolved Photoluminescence. *J. Phys. Chem. C* **2013**, *117*, 25586–25595.
- (43) Mrowetz, M.; Selli, E. Enhanced Photocatalytic Formation of Hydroxyl Radicals on Fluorinated TiO₂. *Phys. Chem. Chem. Phys.* **2005**, *7*, 1100–1102.
- (44) Jańczyk, A.; Krakowska, E.; Stochel, G.; Macyk, W. Singlet Oxygen Photogeneration at Surface Modified Titanium Dioxide. *J. Am. Chem. Soc.* **2006**, *128*, 15574–15575.
- (45) Minella, M.; Faga, M. G.; Maurino, V.; Minero, C.; Pelizzetti, E.; Coluccia, S.; Martra, G. Effect of Fluorination on the Surface Properties of Titania P25 Powder: An FTIR Study. *Langmuir* **2010**, *26*, 2521–2527.
- (46) Barsukov, D. V.; Saprykin, A. V.; Subbotina, I. R.; Usachev, N. Y. Beneficial Effect of TiO₂ Surface Fluorination on the Complete Photooxidation of Ethanol Vapor. *Mendeleev Commun.* **2017**, *27*, 248–250.
- (47) Tang, J.; Quan, H.; Ye, J. Photocatalytic Properties and Photoinduced Hydrophilicity of Surface-Fluorinated TiO₂. *Chem. Mater.* **2007**, *19*, 116–122.
- (48) Mino, L.; Pellegrino, F.; Rades, S.; Radnik, J.; Hodoroba, V. D.; Spoto, G.; Maurino, V.; Martra, G. Beyond Shape Engineering of TiO₂ Nanoparticles: Post-Synthesis Treatment Dependence of Surface Hydration, Hydroxylation, Lewis Acidity and Photocatalytic Activity of TiO₂ Anatase Nanoparticles with Dominant {001} or {101} Facets. *ACS Appl. Nano Mater.* **2018**, *1*, 5355–5365.
- (49) Parrino, F.; Conte, P.; De Pasquale, C.; Laudicina, V. A.; Loddo, V.; Palmisano, L. Influence of Adsorbed Water on the Activation Energy of Model Photocatalytic Reactions. *J. Phys. Chem. C* **2017**, *121*, 2258–2267.
- (50) Fessi, N.; Nsib, M. F.; Cardenas, L.; Guillard, C.; Dapozze, F.; Houas, A.; Parrino, F.; Palmisano, L.; Ledoux, G.; Amans, D.; Chevalier, Y. Surface and Electronic Features of Fluorinated TiO₂ and Their Influence on the Photocatalytic Degradation of 1-Methylnaphthalene. *J. Phys. Chem. C* **2020**, *124*, 11456–11468.
- (51) Khelifi, H.; Parisi, F.; Ellsami, L.; Camera-Roda, G.; Palmisano, L.; Ceccato, R.; Parrino, F. Photocatalytic Partial Oxidation of Tyrosol: Improving the Selectivity Towards Hydrox-

tyrosol by Surface Fluorination of TiO₂. *Top. Catal.* **2020**, DOI: 10.1007/s11244-020-01287-y.

(52) Norris, J. D. Determination of Titanium in Titanium Dioxide Pigments, Paints and Other Materials by Chromium(II) Chloride Reduction and Automatic Potentiometric Titration. *Analyst* **1984**, *109*, 1475–1482.

(53) Camera-Roda, G.; Augugliaro, V.; Cardillo, A. G.; Loddo, V.; Palmisano, L.; Parrino, F.; Santarelli, F. A Reaction Engineering Approach to Kinetic Analysis of Photocatalytic Reactions in Slurry Systems. *Catal. Today* **2016**, *259*, 87–96.

(54) Chen, Y.; Chen, F.; Zhang, J. Effect of Surface Fluorination on the Photocatalytic and Photo-induced Hydrophilic Properties of Porous TiO₂ Films. *Appl. Surf. Sci.* **2009**, *255*, 6290–6296.

(55) Park, J. S.; Choi, W. Enhanced Remote Photocatalytic Oxidation on Surface-Fluorinated TiO₂. *Langmuir* **2004**, *20*, 11523–11527.

(56) Wang, Q.; Chen, C.; Zhao, D.; Ma, W.; Zhao, J. Change of Adsorption Modes of Dyes on Fluorinated TiO₂ and Its Effect on Photocatalytic Degradation of Dyes under Visible Irradiation. *Langmuir* **2008**, *24*, 7338–7345.

(57) Mueller, R.; Kammler, H. K.; Wegner, K.; Pratsinis, S. E. OH Surface Density of SiO₂ and TiO₂ by Thermogravimetric Analysis. *Langmuir* **2003**, *19*, 160–165.

(58) Aveyard, R.; Binks, B. P.; Clint, J. H. Emulsions Stabilized Solely by Colloidal Particles. *Adv. Colloid Interface Sci.* **2003**, *100-102*, 503–546.

(59) Binks, B. P.; Lumsdon, S. O. Influence of Particle Wettability on the Type and Stability of Surfactant-Free Emulsions. *Langmuir* **2000**, *16*, 8622–8631.

(60) Lubansky, A. S.; Yeow, Y. L.; Leong, Y.-K.; Wickramasinghe, S. R.; Han, B. A General Method of Computing the Derivate of Experimental Data. *AIChE J.* **2006**, *52*, 323–332.

(61) Yeow, Y. L.; Wickramasinghe, S. R.; Han, B.; Leong, Y.-K. A New Method of Processing the Time-Concentration Data of Reaction Kinetics. *Chem. Eng. Sci.* **2003**, *58*, 3601–3610.

(62) Kus, M.; Altantzis, T.; Vercauteren, S.; Caretti, I.; Leenaerts, O.; Batenburg, K. J.; Mertens, M.; Meynen, V.; Partoens, B.; Van Doorslaer, S.; Bals, S.; Cool, P. Mechanistic Insight into the Photocatalytic Working of Fluorinated Anatase {001} Nanosheets. *J. Phys. Chem. C* **2017**, *121*, 26275–26286.

(63) Gao, H.; Zhang, D.; Yang, M.; Dong, S. Photocatalytic Behavior of Fluorinated Rutile TiO₂ (110) Surface: Understanding from the Band Model. *Sol. RRL* **2017**, *1*, 1700183.

(64) Boddu, V.; Kim, S.; Adkins, J.; Weimer, E.; Paul, T.; Damavarapu, R. Sensitive Determination of Nitrophenol Isomers by Reverse-Phase High-Performance Liquid Chromatography in Conjunction with Liquid-Liquid Extraction. *Int. J. Environ. Anal. Chem.* **2017**, *97*, 1053–1064.